THE JOURNAL OF BIOLOGICAL CHEMISTRY VOL. 287, NO. 34, pp. 28564–28575, August 17, 2012

The ABCG5 ABCG8 Sterol Transporter Opposes the Development of Fatty Liver Disease and Loss of Glycemic Control Independently of Phytosterol Accumulation*

Received for publication, March 7, 2012, and in revised form, June 16, 2012 Published, JBC Papers in Press, June 19, 2012, DOI 10.1074/jbc.M112.360081

Kai Su[‡§¶], Nadezhda S. Sabeva[‡§¶], Jingjing Liu[‡§¶], Yuhuan Wang[‡§¶], Saloni Bhatnagar[‖], Deneys R. van der Westhuyzen[§¶], and Gregory A. Graf[‡§¶1]**

*From the Departments of [‡]Pharmaceutical Sciences, [‖]Pediatrics, and **Internal Medicine, [§]Graduate Center for Nutritional Sciences, and [¶]Saha Cardiovascular Research Center, University of Kentucky, Lexington, Kentucky 40536*

Background: G5G8 promotes elimination of cholesterol.
Results: The absence of G5G8 accelerates the loss of glycemic control and exacerbates the development of steatosis.
Conclusion: G5G8 mitigates the impact of a high fat diet on hepatic lipid accumulation and glucose intolerance.
Significance: Increased G5G8 in insulin resistance may be an adaptive mechanism that opposes steatosis but increases the risk of cholesterol gallstones.

ABCG5 and ABCG8 form a complex (G5G8) that opposes the absorption of plant sterols but is also expressed in liver where it promotes the excretion of cholesterol into bile. Hepatic G5G8 is transcriptionally regulated by a number of factors implicated in the development of insulin resistance and nonalcoholic fatty liver disease. Therefore, we hypothesized that G5G8 may influence the development of diet-induced obesity phenotypes independently of its role in opposing phytosterol absorption. G5G8 knock-out (KO) mice and their wild type (WT) littermates were challenged with a plant sterol-free low fat or high fat (HF) diet. Weight gain and the rise in fasting glucose were accelerated in G5G8 KO mice following HF feeding. HF-fed G5G8 KO mice had increased liver weight, hepatic lipids, and plasma alanine aminotransferase compared with WT controls. Consistent with the development of nonalcoholic fatty liver disease, macrophage infiltration, the number of TUNEL-positive cells, and the expression of proinflammatory cytokines were also increased in G5G8 KO mice. Hepatic lipid accumulation was associated with increased peroxisome proliferator activated receptor γ, CD36, and fatty acid uptake. Phosphorylation of eukaryotic translation initiation factor 2α (eiF2α) and expression of activating transcription factor 4 and tribbles 3 were elevated in HF-fed G5G8 KO mice, a pathway that links the unfolded protein response to the development of insulin resistance through inhibition of protein kinase B (Akt) phosphorylation. Phosphorylation of Akt and insulin receptor was reduced, whereas serine phosphorylation of insulin receptor substrate 1 was elevated.

ABCG5[2] and *ABCG8* encode a pair of ATP-binding cassette half-transporters that form a complex (G5G8) that opposes the absorption of dietary sterols and promotes the excretion of cholesterol into bile (1–3). Mutations in either *ABCG5* or *ABCG8* result in sitosterolemia (OMIM number 210250), a monogenic recessive disorder characterized by the accumulation of phytosterols in plasma, tendon, and tuberous xanthomas; elevated low density lipoprotein (LDL) cholesterol; and premature coronary artery disease (4–6). The expression of G5G8 is limited to the liver and intestine, suggesting that the phenotypes associated with G5G8 deficiency are a function of excess cholesterol accumulation and the various effects of phytosterols. A partial list of biological activities of phytosterols includes disruptions in nuclear receptor signaling, increased inflammatory gene expression, and the induction of apoptosis (7–10). Inhibition of intestinal sterol absorption with ezetimibe corrects the metabolic phenotypes of a mouse model of sitosterolemia (11). Similarly, ezetimibe has been shown to be effective at lowering plasma phytosterols and LDL cholesterol in sitosterolemic patients, but there are conflicting data on the regression of xanthomas (12–14).

ABCG5 and *ABCG8* are located on opposite strands at 2p21 where expression of both mRNAs is tightly co-regulated due to the sharing of a short intergenic promoter that separates their initiation codons by only 374 base pairs (5, 6, 15). Consistent with a role in opposing excess dietary sterol accumulation, expression of G5G8 mRNAs increases in both liver and intestine in response to cholesterol feeding. Although this effect is lost in mice lacking both liver X receptor (LXR) α and LXRβ, LXR response elements have not been identified within this locus. Nuclear receptors essential for bile acid homeostasis have also been shown to regulate G5G8 expression (15, 16). Hepatocyte nuclear factor 4α cooperates synergistically with either GATA-binding protein 4 or 6 to increase G5G8 expression (17).

* This work was supported, in whole or in part, by National Institutes of Health Grants R01DK080874 (to G. A. G.), 5P20RR021954-05 from the National Center for Research Resources, and 8 P20 GM103527-05 from the NIGMS.
[1] To whom correspondence should be addressed: Dept. of Pharmaceutical Sciences, 345 Biological Pharmaceutical Complex, College of Pharmacy, University of Kentucky, 789 S. Limestone, Lexington, KY 40536-0596. Tel.: 859-257-4749; Fax: 859-257-7564; E-mail: Gregory.Graf@uky.edu.
[2] The abbreviations used are: ABC, ATP-binding cassette; G5, ABCG5; G8, ABCG8; PS, plant sterol; LF, low fat; HF, high fat; ATF, activating transcription factor; Trb3, tribbles 3; NAFLD, nonalcoholic fatty liver disease; Akt, protein kinase B; LXRα, liver X receptor; PPAR, peroxisome proliferator activated receptor; CD36, CD36 antigen; UPR, unfolded protein response; XBP-1, X-box-binding protein-1; GRP78/BiP, glucose-regulated protein 78; FID, flame ionization detection; TG, triglyceride; IRS1, insulin receptor substrate; SR-BI, class B, type I scavenger receptor.

Tissue-specific deletion of hepatic insulin receptor increases G5G8 mRNA through disinhibition of forkhead box protein O1 (FOXO1) (18). The resulting increase in G5G8 and biliary cholesterol concentrations may provide a mechanistic link between insulin resistance and increased risk for cholesterol gallstones. We previously published that G5G8 is down-regulated in liver of both leptin- and leptin receptor-deficient mice, both of which are resistant to cholesterol gallstones despite pronounced insulin resistance (19–21). The functional significance of G5G8 regulation by factors essential for glucose and fatty acid metabolism as well as the disruption of this complex in genetic models of obesity and insulin resistance is unknown.

An emerging body of literature suggests that cholesterol contributes to the development of nonalcoholic fatty liver disease (NAFLD). In LDL receptor-deficient mice, the inclusion of cholesterol in a high fat, high sucrose diet increases the severity of NAFLD, resulting in steatohepatitis (22). In a mouse model of Alström syndrome, the development of NAFLD was associated with the accumulation of hepatic free cholesterol due to an increase in hepatic uptake and a decrease in biliary elimination (23). In this model, hepatic G5G8 was strongly repressed despite the accumulation of hepatic sterols.

We hypothesized that active cholesterol elimination by G5G8 is protective in the development of insulin resistance and fatty liver phenotypes, thus providing a mechanistic link between G5G8 regulation and insulin signaling. To test this hypothesis, we challenged G5G8-deficient mice with high fat diets shown previously to induce insulin resistance and NAFLD. However, phytosterols were recently shown to cause hypertriglyceridemia in G5G8-deficient mice (24). Therefore, we weaned mice onto diets containing ezetimibe to prevent the development of sitosterolemia and eliminated plant sterols from the test diets to prevent the biological activities of phytosterols from confounding our interpretation of the effects of G5G8-dependent cholesterol elimination in the development of insulin resistance and NAFLD.

EXPERIMENTAL PROCEDURES

Animals and Diets

Mice harboring mutant alleles for *Abcg5* and *Abcg8* (B6; 129S6-*Abcg5.Abcg8*^{tm1Hobb}) were obtained from The Jackson Laboratory (Bar Harbor, ME; stock number 004670) and backcrossed for 10 generations to the C57BL/6J strain (stock number 000664). The mutant allele was maintained in the heterozygous state in male mice. Following backcross, strain refreshing to C57BL/6J females obtained from The Jackson Laboratory was conducted every five generations. The colony was maintained in a temperature-controlled room (22 °C) under negative pressure with a 14:10-h (06:00–20:00) light/dark cycle. Mice were housed in individually ventilated cages with free access to food and water and provided enrichment in the form of acrylic houses and nesting material. Mice homozygous for the mutant allele (KO) and their wild type (WT) littermates were obtained from heterozygous, trio matings. Mice utilized in the present study were weaned between 18 and 21 days onto standard rodent chow supplemented with ezetimibe (0.005%) to prevent the accumulation of dietary phytosterols.

At 8 weeks of age, WT and KO male mice (n = 8) were provided free access to a custom formulated low fat (LF; 18% kcal) or high fat (HF; 60% kcal) plant sterol-free diet (Research Diets Inc., New Brunswick, NJ). Macronutrient composition was provided by the supplier; sterol content was determined by GC-MS/FID (Table 1). Formulation of the LF diet required 18% kcal total energy from lard to preclude ω-6 fatty acid deficiency. Diets were replaced weekly to minimize lipid oxidation.

Mice were weighed, fasting glucose levels were recorded, and body composition, including fat mass, lean mass, and free and total water, was measured at initiation (8 weeks) and every 4 weeks of the study in conscious mice using an echoMRI™ whole body composition analyzer (Echo Medical Systems, Houston, TX). A glucose tolerance test was conducted at 22 weeks (14 weeks on diet). An insulin sensitivity test was conducted at 23 weeks (15 weeks on diet). The triglyceride (TG) secretion rate was determined in a separate cohort of mice (n = 4). Mice were injected with 650 mg/kg of body weight Triton WR-1339 (Sigma) via tail vein to block lipoprotein lipase-mediated lipolysis. Blood was collected using heparinized capillary tubes before and 0.5, 1, 2, and 3 h after Triton injection. Total TGs were determined using colorimetric-enzymatic assays (Wako Chemicals, Richmond, VA).

Three days prior to termination of the study, mice were placed in clean cages and individually housed to collect feces for 72 h. On the final day of the study, mice were transferred to individual clean cages, fasted for 4 h to facilitate the collection of gall bladder bile, anesthetized with ketamine:xylazine (9:1, w/w), and analyzed using a Lunar PIXImus II dual energy x-ray absorptiometry scanner to determine femoral length and bone mineral density. Mice were exsanguinated, and tissues were dissected. Tissues were snap frozen in liquid nitrogen, embedded in Tissue-Tek optimal cutting temperature (O.C.T.) compound, and formalin-fixed (10% in phosphate-buffered saline (PBS)) for subsequent analysis. All animal procedures were performed with the approval of the Institutional Animal Care and Use Committee.

Analytical Procedures

Plasma, biliary, dietary, and fecal sterols were analyzed by GC-MS (19). Serum was fractionated by FPLC, and fractions were analyzed for cholesterol content as described previously (19). Fasting glucose level determination, glucose tolerance tests, and area under the curve calculations were conducted as described previously (25). Plasma insulin was measured by ELISA (ALPCO Diagnostics, Salem, NH). Plasma levels of alanine and aspartate aminotransferases were measured using an Infinity AST/ALT liquid stable reagent kit (Thermo Scientific, Waltham, MA).

Liver Histology—Liver was fixed in 10% formalin overnight, transferred to 30% ethanol, and stored at 4 °C. Tissues were subsequently dehydrated, embedded in paraffin, and cut into 5-μm sections. Sections were rehydrated with 0.1 mol/liter PBS (pH 7.4) and stained with hematoxylin and eosin. Collagen was stained using a Trichrome Masson staining kit (Sigma-Aldrich). Cells positive for TUNEL staining were detected with a fluorescein FragEL DNA Fragmentation detection kit (Calbiochem).

Immunofluorescence Microscopy—Mouse liver was dissected and immediately imbedded in optimal cutting temperature (O.C.T.) compound on a block of dry ice. Sections (14 μm) were fixed with methanol (for 5 min at −20 °C), rehydrated in PBS (pH 7.4), and incubated in Buffer A (PBS + 1% BSA (w/v)) at 22 °C for 1 h to reduce nonspecific binding. Sections were incubated with F4/80 antibody (Abcam, San Francisco, CA) at a dilution of 1:200 in Buffer A at 4 °C for 16 h. Sections were washed, mounted in aqueous mounting medium (ProLong Gold antifade reagent with DAPI, Invitrogen), and imaged on a Zeiss Axiovert 200M confocal microscope equipped with an ApoTome.

Hepatic lipids were determined by colorimetric assay following Folch extraction. Approximately 100 mg of liver was ground using a Dounce pestle. Lipids were extracted in 2:1 $CHCl_3$:MeOH at room temperature. The chloroform phase was dried down, solubilized in 1 volume of Triton X-100/$CHCl_3$, dried, and resolubilized in 2 volumes of water. Triglycerides, phospholipids, and total cholesterol were measured with colorimetric kits (Wako Chemicals). The measured values were normalized to the sample weight.

Fecal Neutral Sterols—Total feces from the 72-h period was collected, dried at 37 °C, weighed, and ground to powder. An aliquot of 0.125 g of feces was placed into a glass tube with 1.25 ml of ethanol and 0.25 ml of 10 N NaOH. Lipids were saponified at 72 °C in a water bath for 2 h and extracted (water:ethanol: petroleum ether, 1:1:1, v/v/v). 0.150 mg of 5α-cholestane was used as the internal standard. Following extraction, the organic phase was dried under a steam of nitrogen gas and solubilized in hexane. The amount of neutral sterols (cholesterol, coprostanol, and cholestanol) was quantified by GC-MS/FID.

X-box-binding Protein-1 (XBP-1) Processing: Analysis of XBP-1 mRNA Splicing—Total RNA extraction and cDNA synthesis were carried out as described before. cDNA was amplified with a pair of primers (reverse, 5′-CCA TGG GAA GAT GTT CTG GG-3′and forward, 5′-ACA CGC TTG GGG ATG AAT GC-3′). PCR conditions were as follows: initial denaturation at 94 °C for 3 min followed by 30 cycles of amplification (each with 94 °C for 30 s, 58 °C for 30 s, and 72 °C for 30 s) and a final extension at 72 °C for 3 min. PCR products were analyzed by 2.5% agarose gel electrophoresis (26).

Fatty Acid Uptake—Mouse primary hepatocytes were isolated by liver perfusion with collagenase B and analyzed for fatty acid uptake as described previously (27). Viable hepatocytes were identified by trypan blue exclusion and counted. For the uptake assay, 200 μl of assay buffer (40 μM sodium oleate, 10 μM fatty acid-free bovine serum albumin, 5 μCi/ml [^{3}H]oleate in PBS with 1 mM $MgCl_2$ and 1.2 mM $CaCl_2$) was added to 200 μl of the cell suspension and incubated for various times at 37 °C. Assays were stopped by the addition of 5 ml of ice-cold stop solution (PBS containing 1 mM $MgCl_2$, 1.2 mM $CaCl_2$, 0.1% fatty acid-free bovine serum albumin, and 500 μM phloretin). Cells were pelleted by centrifugation at 500 × *g*, resuspended in 200 μl of water, and analyzed for cell associated-radioactivity by scintillation counting. All assays were performed in duplicate and corrected for the number of viable cells per assay. Nonspecific binding was determined by simultaneous addition of uptake assay buffer and stop solution to 200 μl of the cell suspension on ice. This background value was obtained for each cell preparation and subtracted from all time points.

TABLE 1

Macronutrient and sterol content of standard chow and custom formulated PS-free low and high fat diets

Macronutrient content was provided by the supplier. Sterol content was determined by GC-MS/FID. ND, not detected, or below the limit of detection.

	Standard chow diet	PS-free low fat diet	PS-free high fat diet
Protein (% kcal)	21	21	21
Carbohydrate (% kcal)	68	61	19
Fat (% kcal)	12	18	60
Cholesterol (%)	ND	0.001	0.007
Campesterol (mg/g diet)	0.0680	ND	ND
Stigmasterol (mg/g diet)	0.0566	ND	ND
β-Sitosterol (mg/g diet)	0.5210	ND	ND

Fatty Acid Oxidation—Mouse primary hepatocytes were isolated as above and seeded at a density of 6×10^5 cells/dish onto collagen-coated 35-mm culture dishes. Two days following plating, the cells were analyzed for rates of fatty acid oxidation as described previously with minor modifications (28). Briefly, cells were washed and incubated in serum-free medium containing 0.3 mM unlabeled oleate, 1.0 μCi/ml 9,10-[^{3}H]oleic acid (60 Ci/mmol; PerkinElmer Life Sciences), 2% fatty acid-free BSA, 0.25 mM L-carnitine, and 3 mM glucose for 2, 4, or 6 h at 37 °C. Culture medium was collected, and excess oleate was removed by 2× trichloroacetic acid precipitation (20%). 1 ml of a 2 M KCl, 2 M HCl solution was added to the supernatants (0.5 ml), and radioactive water was extracted twice with 2.5 ml of methanol:chloroform (2:1). The radioactivity in extracts was determined by scintillation counting. Medium incubated in the absence of cells was used to determine the background value, which was subtracted from all values. Total cellular protein was determined, and rates of oxidation were calculated as pmol/h/μg of cell protein.

Statistical Analysis

All statistical analyses were conducted using GraphPad Prism. Data are expressed as mean ± S.E. Data were analyzed by two-way analysis of variance using diet and genotype as factors. Where appropriate, a repeated measure two-way analysis of variance was used within diet to obtain genotype by time interactions. Post hoc comparisons were made using Bonferroni tests. Linear regression was used to determine differences in the rates of TG secretion, fatty acid uptake, and oxidation. Differences were considered significant at $p < 0.05$.

RESULTS

Plasma, Biliary, and Fecal Sterols—To determine whether G5G8 activity opposed the development of diet-induced obesity phenotypes independently of its role in opposing phytosterol accumulation, we challenged G5G8 deficient (KO) mice and their WT littermates with a plant sterol (PS)-free LF or HF diet (Table 1). There was a decrease in biliary cholesterol concentrations and a reduction in fecal neutral sterols in G5G8 KO mice compared with WT controls irrespective of diet (Fig. 1, *A* and *B*). Plasma cholesterol levels were elevated following HF feeding and further increased by the absence of G5G8 (Fig. 1*C*). Phytosterols are easily detected in plasma from WT mice maintained on standard rodent chow but were below the limits of

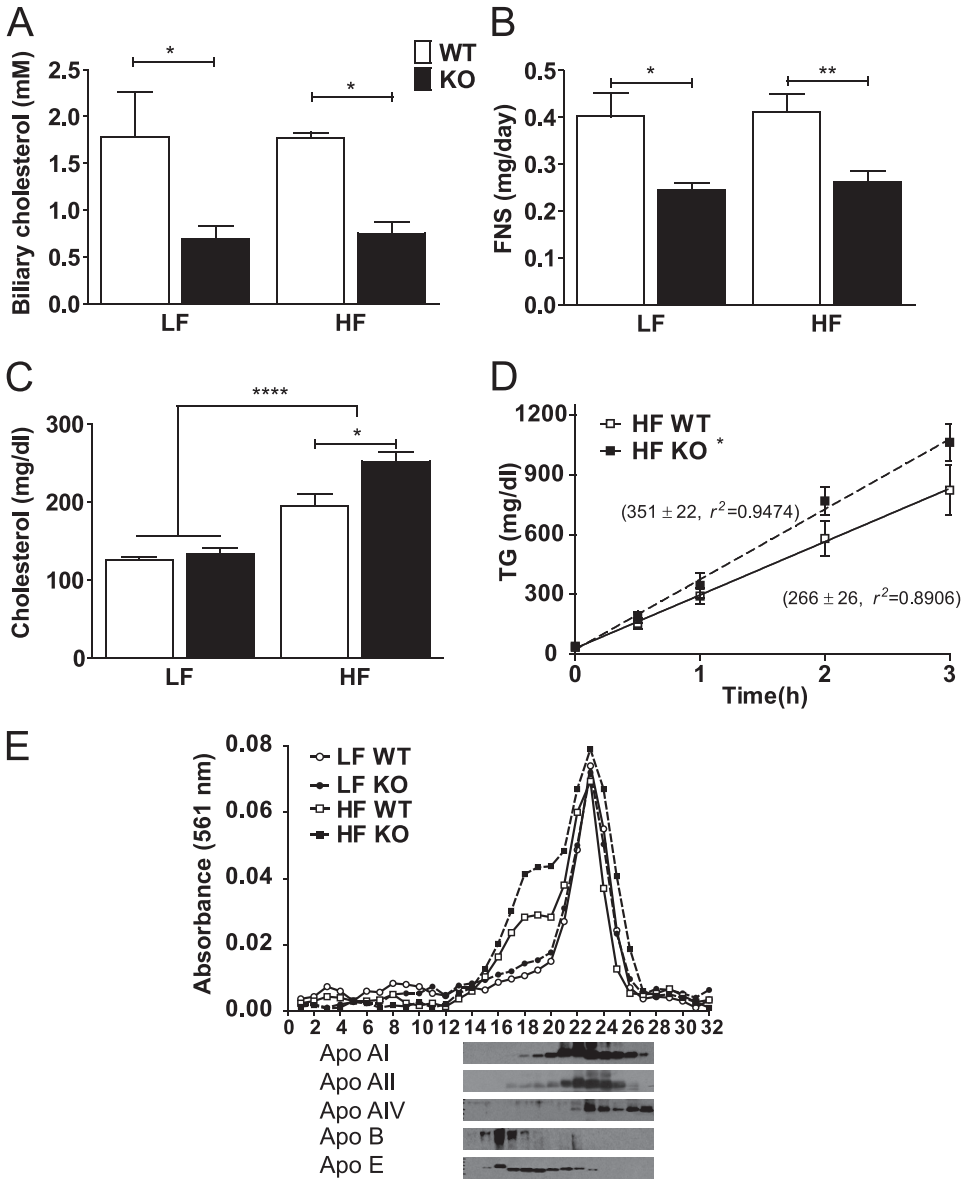

FIGURE 1. **The absence of G5G8 reduces biliary and fecal neutral sterol levels but increases plasma cholesterol following HF feeding.** WT and KO mice were fed a PS-free LF or HF diet. Biliary cholesterol concentrations (*A*) and fecal neutral sterols (*FNS*) (*B*) were determined by GC-MS. *C*, plasma cholesterol levels were determined by enzymatic-colorimetric assays. *D*, linear regression analysis of TG secretion rates (mg/dl/h) for WT and G5G8 KO mice following HF feeding. *E*, pooled serum from three mice in each group was fractionated by FPLC and analyzed for relative cholesterol content. The distribution of apoA-I, apoA-II, apoA-IV, apoB48, and apoE were determined in fractions 14–27 from the G5G8 KO, HF-fed group. Overall effects of diet are indicated by *brackets* terminating in *horizontal lines* over both genotypes. Effects of genotype within each diet are indicated by *bars* terminating in *vertical lines*. Data are the mean ± S.E. (*error bars*) ($n = 8$). *Asterisks* indicate significant differences: *, $p < 0.05$; **, $p < 0.01$; ****, $p < 0.0001$.

detection by GC-MS/FID in all mice examined in the present study (not shown). Although non-fasting TGs tended to be elevated in G5G8 KO mice following HF feeding (37.7 ± 6.3 *versus* 61.4 ± 13 mg/dl, $p = 0.15$), neither fasting nor non-fasting levels differed among genotypes or diets. However, the TG secretion rate was increased in G5G8 KO mice compared with WT controls following HF feeding (Fig. 1*D*). Analysis of FPLC-fractionated plasma indicates that the increase in cholesterol levels in both WT and G5G8 KO mice was predominantly in the LDL and HDL fractions. Immunoblot analysis of fractions 14–27 confirmed that these particles are enriched in apolipoprotein (apo) E and also contain modest amounts of apoA-II and apoA-I (Fig. 1*E*).

Body Weight and Composition—Body weight and composition did not differ between genotypes at 8 weeks of age (Fig. 2). As expected, body weight, fat mass, and to a lesser extent lean mass increased following HF feeding irrespective of genotype. No differences in body composition were observed between genotypes among mice fed LF PS-free diets. Within HF-fed mice, the absence of G5G8 resulted in a modest increase in body weight at 16 and 20 weeks but plateaued after 20 weeks, allowing WT mice to achieve equivalent weight gain by the termination of the study (Fig. 2*A*). Similar results were observed for fat mass (Fig. 2*B*). Lean mass was elevated in HF-fed G5G8 KO mice after only 4 weeks of feeding (12 weeks) and remained significantly elevated throughout the remainder of the study

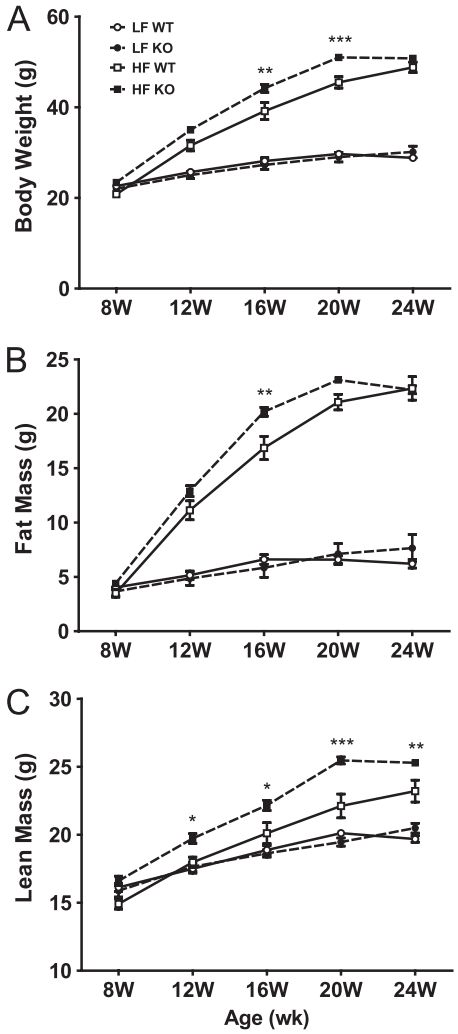

FIGURE 2. **Body weight and body composition in WT and G5G8 KO mice in response to PS-free LF and HF diets.** Body weight (*A*), fat mass (*B*), and lean mass (*C*) were determined by MRI at the initiation of HF and LF diets (8 weeks (*W*)) and every 4 weeks until termination of the experiment (24 weeks). Data are the mean ± S.E. (*error bars*) ($n = 8$). *Asterisks* indicate significant differences between genotypes within diet: *, $p < 0.05$; **, $p < 0.01$; ***, $p < 0.001$.

(Fig. 2*C*). To determine whether the increase in lean mass might be reflective of an overall increase in skeletal size or bone density, mice were analyzed by dual emission x-ray absorptiometry at the termination of the study. Neither femur length nor bone density differed between genotypes of HF-fed mice (not shown).

G5G8 Opposes Steatosis—To determine whether the increase in lean mass was due to hepatomegaly, livers were weighed at dissection. Again, there was an overall effect of diet irrespective of genotype, and no differences between genotypes among LF-fed mice were observed (Fig. 3*A*). Within the HF diet group, the absence of G5G8 resulted in an increase in liver weight as well as liver weight:body weight ratio. When liver weight was deducted from lean mass, no differences in genotype were detected, indicating that hepatomegaly accounts for the increase in lean mass observed in G5G8 KO mice following HF feeding.

Next, we examined liver histology. Whereas no histological differences were appreciated between genotypes on LF diet, the absence of G5G8 resulted in increased vacuolar structures consistent with increased steatosis (Fig. 3*B*). Oil red O staining confirmed the presence of neutral lipid deposition (not shown). Hepatic TG content was increased in both genotypes following HF feeding but was higher in G5G8 KO mice than in WT controls (Fig. 3*C*). A similar pattern was observed for hepatic total, free, and esterified cholesterol (Fig. 3, *D–F*). Given the increase in liver mass in G5G8 KO mice, we calculated the total hepatic pool of TG and cholesterol. The absence of G5G8 resulted in a 2.0-fold increase in the total hepatic TG pool and a 2.5-fold increase in total hepatic cholesterol among HF-fed mice, representing an increase of 75 and 10 mg, respectively.

Increased Fatty Acid Uptake Promotes Steatosis in G5G8 KO Mice—We initially hypothesized that the accumulation of unesterified cholesterol would increase hepatic levels of oxysterols, increase LXR-dependent gene expression, and drive lipogenesis in HF-fed G5G8 KO mice. Therefore, we examined the expression levels of LXR isoforms as well as LXR target genes (Table 2). Both LXRα and -β were modestly suppressed by HF diet regardless of genotype. LXR target genes that promote lipogenesis, including sterol response element-binding protein-1, acetyl-CoA carboxylase, and fatty-acid synthase were unaffected by diet, genotype, or their interaction. Although mRNA levels for stearoyl-CoA desaturase-1 were increased by 80% in HF-fed G5G8 KO mice compared with WT controls, additional LXR target genes involved in sterol efflux (ATP-binding cassette, subfamily A (ABCA1)) and metabolism to primary bile acids (cytochrome P450, family 7, subfamily a, polypeptide 1 (CYP7A1)) were also unaffected. Collectively, the data do not support a role for enhanced LXR signaling as the mechanism for elevated hepatic steatosis in G5G8 KO mice following HF feeding.

A second potential mechanism for hepatic TG accumulation is impaired VLDL secretion. However, there was no reduction in microsomal triglyceride transfer protein, and TG secretion rates in HF-fed G5G8 KO mice were slightly elevated (Fig. 1), indicating that impaired VLDL secretion cannot account for enhanced steatosis.

To determine whether enhanced fatty acid uptake and storage might contribute to hepatic TG accumulation, the peroxisome proliferator-activated receptor γ (PPARγ) pathway was analyzed. PPARγ mRNA increased following high fat feeding and was greater in magnitude in G5G8 KO mice compared with WT controls (Table 2). There was also a further increase in CD36 and fatty acid-binding protein 4 (aP2) in G5G8 KO mice. Although the expression of very low density lipoprotein receptor tended to be higher in G5G8 KO mice, this difference did not reach statistical significance. The increase in CD36 was confirmed by immunoblot analysis (Fig. 4*A*). To determine whether the increase in CD36 protein was associated with enhanced fatty acid uptake, primary hepatocytes isolated from HF-fed WT and G5G8 KO mice were analyzed for rates of oleate uptake and incorporation (Fig. 4*B*). Fatty acid uptake was increased by 45% in G5G8 KO mice compared with WT controls. These data suggest that activation of PPARγ facilitates hepatic fatty acid uptake and storage and contributes to enhanced TG accumulation in G5G8 KO mice.

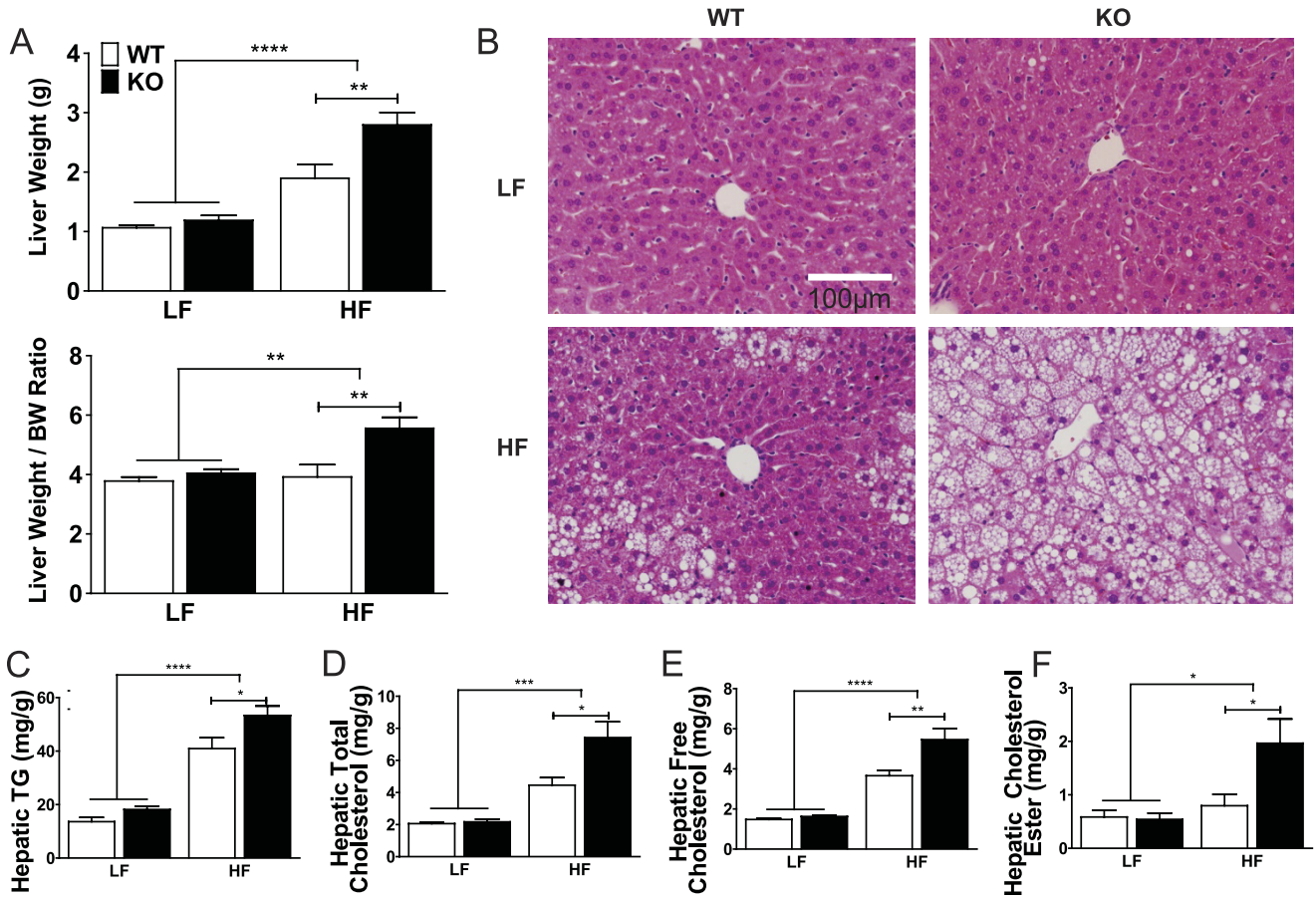

FIGURE 3. **Liver weight, histology, and lipids in WT and G5G8 KO mice in response to PS-free LF and HF diets.** *A*, total liver weight and liver weight to body weight (*BW*) ratio. *B*, formalin-fixed liver sections stained with hematoxylin and eosin. *C–F*, hepatic triglycerides and total, free, and esterified cholesterol per gram of wet tissue weight. Overall effects of diet are indicated by *brackets* terminating in *horizontal lines* over both genotypes. Effects of genotype within each diet are indicated by *bars* terminating in *vertical lines*. Data are the mean ± S.E. (*error bars*) ($n = 8$). *Asterisks* indicate significant differences: *, $p < 0.05$; **, $p < 0.01$; ***, $p < 0.001$; ****, $p < 0.0001$.

TABLE 2

Relative mRNA abundance for selected genes

SREBP-1, sterol response element-binding protein-1; ACC-1, acetyl-CoA carboxylase; FAS, fatty-acid synthase; SCD-1, stearoyl-CoA desaturase-1; CYP7A1, cytochrome P450, family 7, subfamily a, polypeptide 1; ABCA1, ATP-binding cassette, subfamily A; ACOX1, acyl-CoA oxidase 1; CPT1A, carnitine palmitoyltransferase 1A; aP2, fatty acid-binding protein 4; VLDLR, very low density lipoprotein receptor; MTTP, microsomal triglyceride transfer protein.

Gene	Diet	LF		HF	
		WT	KO	WT	KO
LXRα	[a]	1.00 ± 0.03	0.90 ± 0.03	0.87 ± 0.03	0.82 ± 0.04
LXRβ	[b]	1.00 ± 0.03	0.93 ± 0.04	0.65 ± 0.03	0.65 ± 0.03
SREBP-1		1.01 ± 0.06	1.12 ± 0.09	1.10 ± 0.13	1.08 ± 0.09
ACC-1		1.04 ± 0.13	1.13 ± 0.17	0.76 ± 0.09	0.92 ± 0.06
FAS		1.05 ± 0.13	1.83 ± 0.48	1.81 ± 0.32	2.03 ± 0.26
SCD-1		1.05 ± 0.14	1.42 ± 0.20	1.04 ± 0.23	1.85 ± 0.23[c]
CYP7A1		1.04 ± 0.13	1.27 ± 0.12	1.79 ± 0.44	0.69 ± 0.23[c]
ABCA1		1.02 ± 0.11	0.99 ± 0.09	0.93 ± 0.05	0.82 ± 0.07
MTTP	[a]	1.02 ± 0.09	0.98 ± 0.04	0.82 ± 0.05	0.74 ± 0.03
PPARγ	[d]	1.00 ± 0.04	1.32 ± 0.31	1.88 ± 0.10	2.53 ± 0.11[c]
CD36	[d]	1.02 ± 0.10	2.34 ± 0.61	4.55 ± 0.44	7.22 ± 0.25[e]
aP2	[d]	1.01 ± 0.08	1.31 ± 0.06	2.42 ± 0.47	3.67 ± 0.23[c]
VLDLR	[d]	1.06 ± 0.16	1.38 ± 0.50	7.63 ± 0.93	8.83 ± 0.96
PPARα		1.03 ± 0.11	0.98 ± 0.06	0.96 ± 0.05	0.79 ± 0.06
ACOX1		1.01 ± 0.07	1.13 ± 0.13	1.24 ± 0.08	1.09 ± 0.05
CPT1A	[f]	1.01 ± 0.06	1.33 ± 0.20	1.22 ± 0.10	1.83 ± 0.22[c]

[a] Indicates main effect of diet irrespective of genotype at $p < 0.01$.
[b] Indicates main effect of diet irrespective of genotype at $p < 0.001$.
[c] Significant difference at $p < 0.05$.
[d] Significant difference between diets within genotype at $p < 0.0001$.
[e] Significant difference at $p < 0.001$.
[f] Significant difference between diets within genotype at $p < 0.05$.

Finally, we evaluated genes involved in fatty acid oxidation to determine whether a reduction may also contribute to the fatty liver phenotype in HF-fed G5G8 KO mice. PPARα and selected target genes that promote fatty acid oxidation, acyl-CoA oxidase 1, and carnitine palmitoyltransferase 1A, were not reduced by the absence of G5G8 in HF-fed mice (Table 2). Consistent with these findings, we failed to detect differences in the rate of fatty acid oxidation in primary hepatocytes isolated from HF-fed WT and G5G8 KO mice (Fig. 4*C*).

G5G8 Is Protective in NAFLD—To determine whether steatosis had progressed to nonalcoholic steatohepatitis, we first measured plasma levels of liver enzymes (Fig. 5, *A* and *B*). Serum alanine aminotransferase and aspartate aminotransferase levels were unaffected by G5G8 deficiency in LF-fed mice but were increased by HF diet. Hepatic expression of tumor necrosis factor-α (TNF-α), monocyte chemoattractant protein-1, and interleukin-1β (IL-1β) were each elevated in G5G8 KO mice compared with WT controls on HF diet (Fig. 5*C*). Some histological indicators of nonalcoholic steatohepatitis were also exacerbated by G5G8 deficiency among HF-fed mice, including macrophage infiltration and apoptosis as judged by F4/80 and TUNEL staining, respectively (Fig. 5, *D* and *E*). However, we did not observe evidence of fibrosis (not shown).

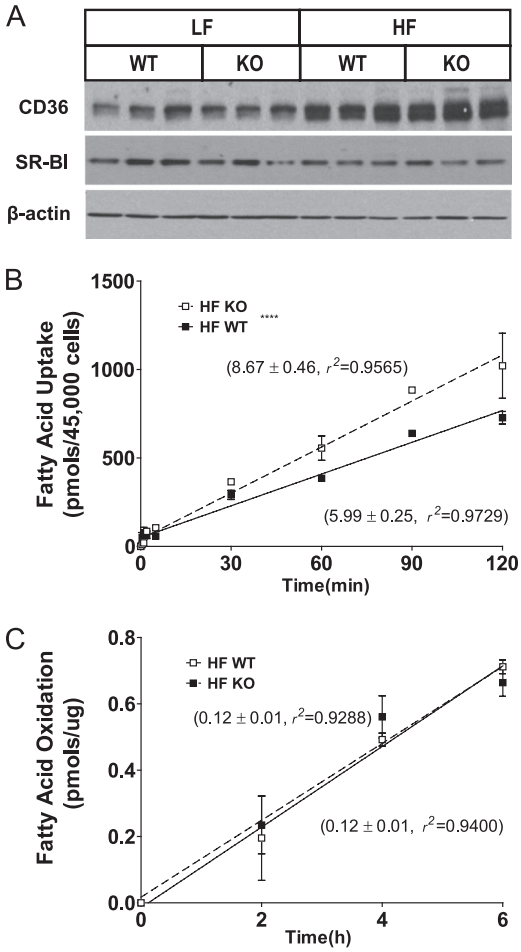

FIGURE 4. **Class B scavenger receptor expression in liver and fatty acid uptake and oxidation in primary hepatocytes in WT and G5G8 KO mice in response to PS-free HF diet.** *A*, immunoblot analysis of the CD36 and SR-BI. β-Actin was used as a loading control. Linear regression analysis of fatty acid uptake (*B*) and fatty acid oxidation (*C*) in mouse primary hepatocytes isolated from WT and G5G8 KO mice following 8 weeks of feeding the PS-free HF diet. Values adjacent to *lines* indicate the slope and coefficient of determination (r^2) for each regression line. **** indicates that the slopes of the regression lines are significantly different ($p < 0.0001$).

G5G8 Mitigates the Loss of Glycemic Control and Insulin Resistance—The development of fatty liver disease is associated with the loss of glycemic control and hepatic insulin resistance. The absence of G5G8 alone had no effect on fasting glucose levels in mice at 8–24 weeks of age on low fat diet (Fig. 6*A*). However, HF feeding increased fasting glucose levels in G5G8 KO but not WT mice at 16 weeks. At 20 weeks, fasting glucose in HF-fed mice was elevated in both genotypes compared with LF controls but further increased in G5G8 KO mice. As with body weight and fat mass, fasting glucose levels plateaued in G5G8 KO mice and were equivalent between genotypes by the end of the study.

Consistent with the development of insulin resistance in response to HF diets, fasting levels of insulin were elevated in HF-fed mice irrespective of genotype at the termination of the study (Fig. 6*B*). Among HF-fed mice, the absence of G5G8 further increased fasting insulin levels. A glucose tolerance test was conducted at 22 weeks (Fig. 6*C*). Similar to elevated insulin, HF diets decreased glucose tolerance regardless of genotype. Among HF-fed mice, the absence of G5G8 tended to increase blood glucose levels at all time points but was only significant at 30 min. Analysis of the area under the curves indicates an overall effect of diet and a further increase in G5G8 KO mice (Fig. 6*D*). An insulin sensitivity test was conducted in HF-fed mice at 23 weeks (Fig. 6*E*). A main effect of genotype was detected in the two-way analysis of variance, but Bonferroni post hoc comparisons failed to detect significant differences at individual time points. Similar to the glucose tolerance test, a modest but significant difference was detected in the area under the curves between HF-fed G5G8 KO and WT controls (Fig. 6*E*).

Unfolded Protein Response (UPR) Links Hepatic Cholesterol to Insulin Resistance—Elevations in cellular cholesterol have been shown to activate the UPR (also commonly called the endoplasmic reticulum stress response) in cultured macrophages (29). A growing body of literature has tied the UPR to the development of fatty liver disease and insulin resistance (30). To determine whether the increase in hepatic free cholesterol in G5G8 KO mice was associated with activation of the UPR among HF-fed mice, we assessed measures of each of the three arms of the UPR. Consistent with activation of the UPR, phosphorylation of eukaryotic initiation factor 2α (eiF2α) was significantly increased (Fig. 7, *A* and *B*). Initiation of the UPR also includes activation of the endonuclease inositol-requiring enzyme 1, which promotes alternative splicing of XBP-1 mRNA to generate spliced XBP-1. We used an RT-PCR method and traditional agarose gel electrophoresis but saw no evidence of increased spliced XBP-1 with either method (Fig. 7*C*). The third component of the UPR is the release of activating transcription factor-6α (ATF6α) from the endoplasmic reticulum and its cleavage in the Golgi to release the transcriptionally active, nuclear form of the protein. We observed no evidence for increased levels of mRNAs for the ATF6 target genes XBP-1 and glucose-regulated protein 78 (GRP78/BiP). Immunoblot analysis confirmed these results for GRP78 and another ATF6 target gene, GRP94, which was slightly reduced in G5G8 KO mice.

Activation of tribbles 3 (Trb3) down-regulates protein kinase B (Akt) signaling and has been linked to the development of hepatic insulin resistance (31). To confirm enhanced downstream signaling following inhibition of eiF2α by phosphorylation, we measured mRNA levels for ATF4 and Trb3. There was a modest but significant increase in ATF4 mRNA and a 2-fold increase in Trb3 mRNA. Immunoblotting confirmed a similar increase in levels of Trb3 protein in HF-fed G5G8 KO mice compared with WT controls. Consistent with the role of Trb3 in the development of insulin resistance, we also observed a reduction in phosphorylated Akt.

We also probed upstream of Akt in the insulin signaling pathway. Analysis of total and phosphorylated insulin receptor indicated a modest reduction in phospho-insulin receptor (Fig. 7, *A* and *B*). Tyrosine phosphorylation of the insulin receptor substrate (IRS1) was below the limit of detection in these non-stimulated samples, but we were able to detect an increase in serine phosphorylated IRS1, suggesting that additional mechanisms may also contribute to the loss of glycemic control in HF-fed G5G8 KO mice.

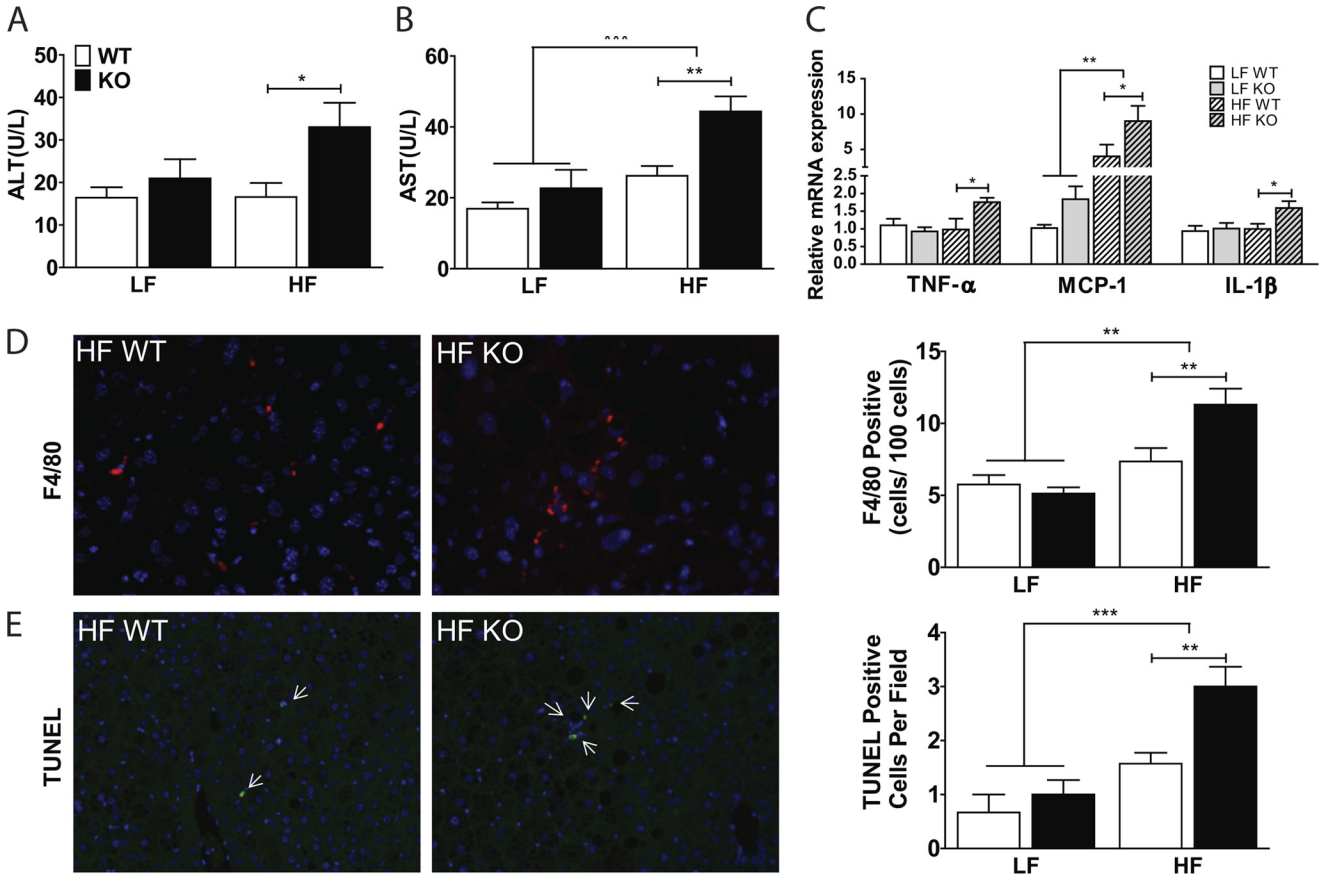

FIGURE 5. **Inflammation, macrophage infiltration, and apoptosis in liver of WT and G5G8 KO mice in response to PS-free LF and HF diets.** Plasma levels of alanine aminotransferase (*ALT*; *A*) and aspartate aminotransferase (*AST*; *B*) were determined by commercial assays. *U*, units. *C*, inflammatory gene expression in liver was determined by quantitative RT-PCR. Data are the mean ± S.E. (*error bars*) ($n = 8$). Overall effects of diet are indicated by *brackets* terminating in *horizontal lines* over both genotypes. Effects of genotype within each diet are indicated by *bars* terminating in *vertical lines*. *Asterisks* indicate significant differences: *, $p < 0.05$; **, $p < 0.01$. *D*, macrophage infiltration in HF-fed mice as determined by the number of F4/80-positive cells. *E*, TUNEL-positive cells (*arrows*) in liver of WT and G5G8 KO mice maintained on HF diet. Data are the mean ± S.E. (*error bars*) from 10 randomly chosen fields from two mice in each group. Data were quantified using the automeasure function in Axiovision 4.8 software. **, $p < 0.01$; ***, $p < 0.001$.

DISCUSSION

The key finding of the present study is that G5G8 plays a previously unappreciated, protective role in the development of NAFLD and the maintenance of glycemic control in a mouse model of diet-induced obesity. These effects were independent of the accumulation of biologically active phytosterols, revealing that active elimination of cholesterol by the G5G8 sterol transporter is essential for hepatic cholesterol homeostasis in the setting of obesity. However, it is important to note that differences in body weight, fat mass, and fasting glucose were most robust relatively early in the HF feeding period and that by the end of the study many of these parameters did not differ between genotypes. Thus, G5G8 activity opposes and can delay metabolic phenotypes associated with HF diets but is insufficient to prevent the complete manifestation of most obesity-related phenotypes. Whether accelerating G5G8-dependent cholesterol elimination can reverse metabolic phenotypes associated with obesity and NAFLD remains to be determined.

Cholesterol Homeostasis—The role of G5G8 in opposing the accumulation of dietary sterols is well established. The absence of G5G8 increases both cholesterol and phytosterol absorption (32). Conversely, expression of a G5G8 transgene reduces cholesterol absorption as well as plasma cholesterol and atherosclerosis in LDL receptor-deficient mice (2, 33). Although G5G8 clearly plays a major role in biliary cholesterol elimination, metabolic phenotypes associated with G5G8 deficiency are resolved when sterol absorption is blocked in mice (11). The present study confirms and extends the findings of this earlier report when plant sterol accumulation is prevented by elimination from the diet. Although we have not conducted a thorough and quantitative study, fertility is also restored in G5G8 KO mice maintained on PS-free diets.[3] These observations indicate that in the absence of additional perturbations in lipid metabolism sterol homeostasis can be maintained through some combination of reduced synthesis, increased conversion to bile acids, and accelerated transintestinal cholesterol elimination in the absence of G5G8. With respect to transintestinal cholesterol elimination, it should be noted that the reduction in fecal neutral sterols observed in the present study is inconsistent with observations from this and other models of G5G8 deficiency in mice (for a review, see Ref. 34). Although the diet used in the present study is distinct from previous reports, the reason for this difference is unknown.

[3] K. Su, N. S. Sabeva, J. Liu, Y. Wang, S. Bhatnagar, D. R. van der Westhuyzen, and G. A. Graf, unpublished observation.

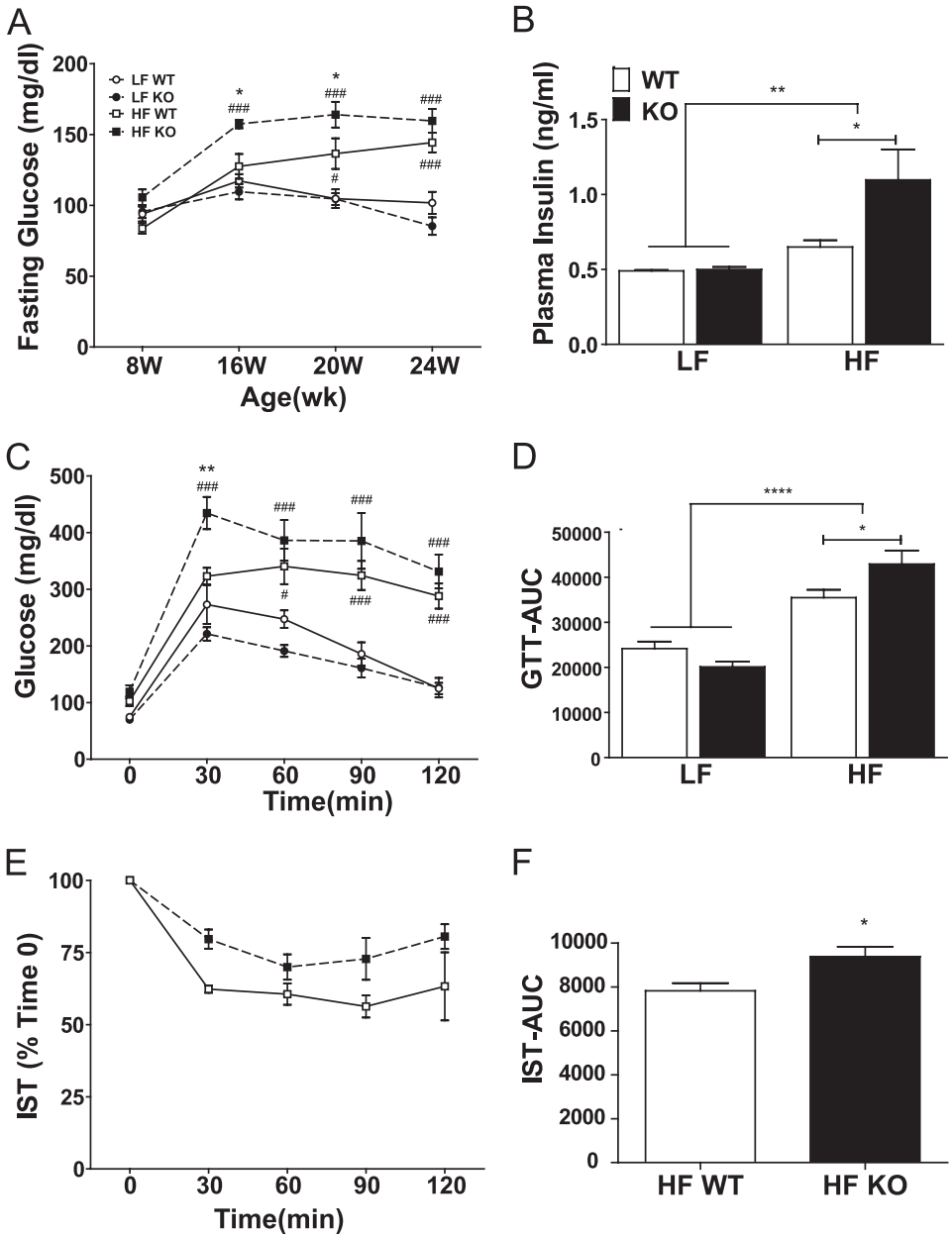

FIGURE 6. **Measures of glycemic control in WT and G5G8 KO mice in response to PS-free LF and HF diets.** *A*, fasting glucose was determined at the initiation of HF and LF diets (8 weeks (*W*)) and every 4 weeks until termination of the experiment (24 weeks). *B*, plasma insulin levels were determined at termination of the study. *C*, a glucose tolerance test was conducted at 22 weeks. *D*, area under the curve (*AUC*) for blood glucose during the glucose tolerance test (*GTT*) was calculated for individual mice from the data in *C*. *E*, an insulin sensitivity test (*IST*) was conducted at 23 weeks in HF-fed mice only. *F*, area under the curve for blood glucose during the insulin sensitivity test was calculated for individual mice from the data in *E*. Overall effects of diet are indicated by *brackets* terminating in *horizontal lines* over both genotypes. Effects of genotype within each diet are indicated by *bars* terminating in *vertical lines*. Data are mean ± S.E. (*error bars*) ($n = 8$). *Asterisks* indicate significant differences: *, $p < 0.05$; **, $p < 0.01$; ****, $p < 0.0001$. *Pound signs* indicate significant differences between diets within genotype: #, $p < 0.05$; ###, $p < 0.001$.

Cholesterol and NAFLD—The protective effect of G5G8 in NAFLD is presumably due to its role in biliary cholesterol excretion. However, dietary cholesterol has been shown to contribute to the development of nonalcoholic steatohepatitis in LDL receptor-deficient mice (22). Conversely, a growing body of literature indicates that inhibition of cholesterol absorption is protective in the development of NAFLD and cholesterol gallstones (35). Consequently, it is important to note that cholesterol levels are higher in the HF diet than in the LF diet or in standard rodent chow. Although these levels are substantially lower (0.007%) than generally used in cholesterol feeding studies (0.15–2.0%), there may be a role for dietary cholesterol and intestinal G5G8 activity in the development of NAFLD in G5G8 KO mice. In the absence of a tissue-specific model for G5G8 deficiency, studies that block cholesterol absorption altogether or normalize cholesterol between diets will be required to determine the role of intestinal G5G8 activity in opposing NAFLD.

The molecular mechanisms that link hepatic cholesterol accumulation to enhanced NAFLD in G5G8 KO mice were not expected. Cholesterol feeding results in the accumulation of oxysterols and increased expression of LXR target genes,

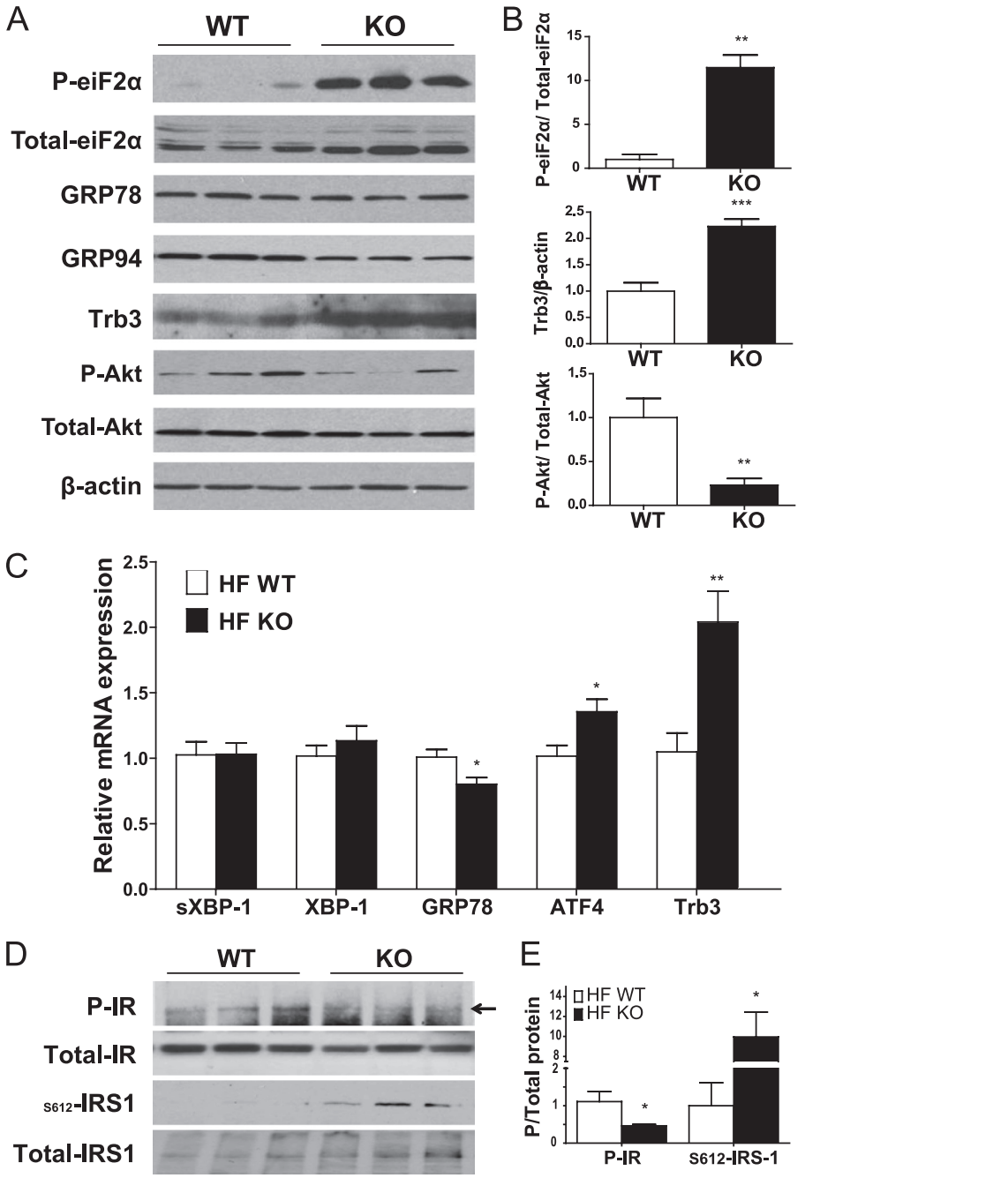

FIGURE 7. **Activation of the PERK arm of the UPR in liver of high fat-fed WT and G5G8 KO mice.** *A*, immunoblot analysis of total and phospho-eiF2α (*P-eiF2α*), GRP78, GRP94, Trb3, and total and phospho-Akt (*P-Akt*). *B* and *E*, total protein or β-actin was used as a loading control for densitometric analysis of signal intensities for six mice in each group. *C*, quantitative RT-PCR was used to determine mRNA levels for spliced XBP-1 (*sXBP-1*) and total XBP-1, GRP78, ATF4, and Trb3. Data are mean ± S.E. (*error bars*) ($n = 6$). *Asterisks* indicate significant differences at $p < 0.05$ (*), $p < 0.01$ (**), and $p < 0.001$ (***) using an unpaired, two-tailed *t* test. *D*, immunoblot analysis of total and phospho-insulin receptor (*P-IR*) and total and serine 612 phosphorylated IRS1 ($_{S612}$*-IRS1*). An *arrow* denotes the phospho-insulin receptor-specific band. Samples are from three randomly selected HF-fed WT and G5G8 KO mice collected following a 4-h fast beginning at lights-on.

including those involved in lipogenesis. Despite the increased accumulation of both free and esterified cholesterol in the liver, we saw no evidence for increased LXR signaling in G5G8 KO compared with WT mice on HF diets. It is possible that the expression of these genes was elevated during the early phases of adipose expansion but normalized by the termination of the study. Indices for the loss of glycemic control and increased fat mass in G5G8 KO mice were evident at 16 and 20 weeks, but by the termination of the study, WT mice achieved similar levels. Alternatively, cholesterol destined for secretion by G5G8 may be protected from oxysterol-generating enzymes, thereby masking hepatic cholesterol accumulation from LXR.

Hepatic intracellular cholesterol trafficking is poorly understood, and neither the pools nor the routes for sterol delivery to G5G8 are known. HDL cholesterol has been shown to directly contribute to biliary cholesterol excretion (36, 37). In mice, this pathway is dependent on the activity of the class B, type I scavenger receptor (SR-BI), which is essential for delivery of HDL

cholesterol to the liver and directly contributes to biliary cholesterol elimination (38–40). In the present study, we observed an accumulation of large, apoE-enriched HDL consistent with decreased SR-BI activity. Although we did not observe a decrease in SR-BI protein, SR-BI surface localization is dependent upon insulin signaling (41). Consequently, the development of insulin resistance may have compromised SR-BI activity without a concomitant reduction in protein.

Beyond lipogenesis, additional mechanisms that can potentially contribute to hepatic lipid accumulation include decreased TG secretion, decreased fatty acid oxidation, and enhanced storage. We did not observe a decrease in TG secretion in G5G8 KO mice (Fig. 1) nor did we observe reductions in mRNAs for PPARα and PPARα target genes or rates of fatty acid oxidation in primary hepatocytes. Rather, we observed an increase in PPARγ and several of its target genes, including CD36. Consistent with this mechanism for enhanced steatosis in HF-fed G5G8 KO mice, fatty acid uptake was elevated in primary hepatocytes isolated from HF-fed G5G8 KO mice compared with WT controls. Although these changes were associated with enhanced lipid accumulation, they may be reflective of the extent of NAFLD rather than causative. Consequently, the precise molecular mechanisms that link G5G8 deficiency to hepatic TG accumulation remain unclear.

G5G8, Cholesterol, and eiF2α—The UPR is thought to play a major role in the development of hepatic insulin resistance and NAFLD (30). Cholesterol accumulation is an activator of the UPR in cultured macrophages (29). Therefore, it seemed plausible that the accumulation of cholesterol in liver might activate the UPR as a mechanism that linked G5G8 deficiency to the rapid loss of glycemic control. However, most components of the UPR were not affected by the absence of G5G8. There was no apparent change in the activity of IRE-1 based on the appearance of spliced XBP-1. Likewise, we observed no differences in mRNAs for ATF6 target genes, indicating that the precursor was sufficiently retained in the endoplasmic reticulum to prevent increases in transcriptional activity. We did observe robust phosphorylation of eiF2α as well as increased mRNAs for ATF4 and Trb3. Trb3 protein was elevated, and there was a reduction in Akt phosphorylation, providing a mechanistic link to accelerated loss of glycemic control and hepatic insulin resistance in G5G8 KO mice.

We also probed upstream of Akt in the insulin signaling pathway. Serine phosphorylation of IRS1 was clearly increased, and a reduction in tyrosine phosphorylated insulin receptor was detected. Although these tissues were collected following a 4-h fast and were not stimulated with exogenous insulin, it is noteworthy that insulin levels in serum collected simultaneously were elevated in HF-fed G5G8 KO mice compared with WT controls.

It remains unclear how the loss of G5G8 activity leads to eiF2α phosphorylation. In the present study, this was limited to the eiF2α arm of the UPR pathway. Whether the activation of pancreatic eif2-alpha kinase (PERK) is particularly sensitive to cellular free sterol levels or whether other kinases shown to increase eiF2α phosphorylation in response to limitations in amino acids or heme or perhaps other cellular stressors are involved remain to be determined.

Acknowledgments—We thank Alan Daugherty and Deborah Howatt within the Saha Cardiovascular Research Center, University of Kentucky for assistance with FPLC analysis of serum and Wendy Katz within the Graduate Center for Nutritional Sciences for assistance with histological analyses. We also thank Maria Hatzoglou (Case Western Reserve) for helpful discussions concerning the activation of the UPR.

REFERENCES

1. Graf, G. A., Li, W. P., Gerard, R. D., Gelissen, I., White, A., Cohen, J. C., and Hobbs, H. H. (2002) Coexpression of ATP-binding cassette proteins ABCG5 and ABCG8 permits their transport to the apical surface. *J. Clin. Investig.* **110,** 659–669
2. Yu, L., Li-Hawkins, J., Hammer, R. E., Berge, K. E., Horton, J. D., Cohen, J. C., and Hobbs, H. H. (2002) Overexpression of ABCG5 and ABCG8 promotes biliary cholesterol secretion and reduces fractional absorption of dietary cholesterol. *J. Clin. Investig.* **110,** 671–680
3. Graf, G. A., Yu, L., Li, W. P., Gerard, R., Tuma, P. L., Cohen, J. C., and Hobbs, H. H. (2003) ABCG5 and ABCG8 are obligate heterodimers for protein trafficking and biliary cholesterol excretion. *J. Biol. Chem.* **278,** 48275–48282
4. Salen, G., Shefer, S., Nguyen, L., Ness, G. C., Tint, G. S., and Shore, V. (1992) Sitosterolemia. *J. Lipid Res.* **33,** 945–955
5. Berge, K. E., Tian, H., Graf, G. A., Yu, L., Grishin, N. V., Schultz, J., Kwiterovich, P., Shan, B., Barnes, R., and Hobbs, H. H. (2000) Accumulation of dietary cholesterol in sitosterolemia caused by mutations in adjacent ABC transporters. *Science* **290,** 1771–1775
6. Lee, M. H., Lu, K., Hazard, S., Yu, H., Shulenin, S., Hidaka, H., Kojima, H., Allikmets, R., Sakuma, N., Pegoraro, R., Srivastava, A. K., Salen, G., Dean, M., and Patel, S. B. (2001) Identification of a gene, ABCG5, important in the regulation of dietary cholesterol absorption. *Nat. Genet.* **27,** 79–83
7. Sabeva, N. S., McPhaul, C. M., Li, X., Cory, T. J., Feola, D. J., and Graf, G. A. (2011) Phytosterols differentially influence ABC transporter expression, cholesterol efflux and inflammatory cytokine secretion in macrophage foam cells. *J. Nutr. Biochem.* **22,** 777–783
8. Bao, L., Li, Y., Deng, S. X., Landry, D., and Tabas, I. (2006) Sitosterol-containing lipoproteins trigger free sterol-induced caspase-independent death in ACAT-competent macrophages. *J. Biol. Chem.* **281,** 33635–33649
9. Yang, C., Yu, L., Li, W., Xu, F., Cohen, J. C., and Hobbs, H. H. (2004) Disruption of cholesterol homeostasis by plant sterols. *J. Clin. Investig.* **114,** 813–822
10. Carter, B. A., Taylor, O. A., Prendergast, D. R., Zimmerman, T. L., Von Furstenberg, R., Moore, D. D., and Karpen, S. J. (2007) Stigmasterol, a soy lipid-derived phytosterol, is an antagonist of the bile acid nuclear receptor FXR. *Pediatr. Res.* **62,** 301–306
11. Yu, L., von Bergmann, K., Lütjohann, D., Hobbs, H. H., and Cohen, J. C. (2005) Ezetimibe normalizes metabolic defects in mice lacking ABCG5 and ABCG8. *J. Lipid Res.* **46,** 1739–1744
12. Salen, G., Starc, T., Sisk, C. M., and Patel, S. B. (2006) Intestinal cholesterol absorption inhibitor ezetimibe added to cholestyramine for sitosterolemia and xanthomatosis. *Gastroenterology* **130,** 1853–1857
13. Salen, G., von Bergmann, K., Lütjohann, D., Kwiterovich, P., Kane, J., Patel, S. B., Musliner, T., Stein, P., Musser, B., and Multicenter Sitosterolemia Study Group (2004) Ezetimibe effectively reduces plasma plant sterols in patients with sitosterolemia. *Circulation* **109,** 966–971
14. Lütjohann, D., von Bergmann, K., Sirah, W., Macdonell, G., Johnson-Levonas, A. O., Shah, A., Lin, J., Sapre, A., and Musliner, T. (2008) Long-term efficacy and safety of ezetimibe 10 mg in patients with homozygous sitosterolemia: a 2-year, open-label extension study. *Int. J. Clin. Pract.* **62,** 1499–1510
15. Freeman, L. A., Kennedy, A., Wu, J., Bark, S., Remaley, A. T., Santamarina-Fojo, S., and Brewer, H. B., Jr. (2004) The orphan nuclear receptor LRH-1 activates the ABCG5/ABCG8 intergenic promoter. *J. Lipid Res.* **45,** 1197–1206

16. Repa, J. J., Berge, K. E., Pomajzl, C., Richardson, J. A., Hobbs, H., and Mangelsdorf, D. J. (2002) Regulation of ATP-binding cassette sterol transporters ABCG5 and ABCG8 by the liver X receptors α and β. *J. Biol. Chem.* **277,** 18793–18800
17. Sumi, K., Tanaka, T., Uchida, A., Magoori, K., Urashima, Y., Ohashi, R., Ohguchi, H., Okamura, M., Kudo, H., Daigo, K., Maejima, T., Kojima, N., Sakakibara, I., Jiang, S., Hasegawa, G., Kim, I., Osborne, T. F., Naito, M., Gonzalez, F. J., Hamakubo, T., Kodama, T., and Sakai, J. (2007) Cooperative interaction between hepatocyte nuclear factor 4α and GATA transcription factors regulates ATP-binding cassette sterol transporters ABCG5 and ABCG8. *Mol. Cell. Biol.* **27,** 4248–4260
18. Biddinger, S. B., Haas, J. T., Yu, B. B., Bezy, O., Jing, E., Zhang, W., Unterman, T. G., Carey, M. C., and Kahn, C. R. (2008) Hepatic insulin resistance directly promotes formation of cholesterol gallstones. *Nat. Med.* **14,** 778–782
19. Sabeva, N. S., Rouse, E. J., and Graf, G. A. (2007) Defects in the leptin axis reduce abundance of the ABCG5-ABCG8 sterol transporter in liver. *J. Biol. Chem.* **282,** 22397–22405
20. Graewin, S. J., Lee, K. H., Tran, K. Q., Goldblatt, M. I., Svatek, C. L., Nakeeb, A., and Pitt, H. A. (2004) Leptin-resistant obese mice do not form biliary crystals on a high cholesterol diet. *J. Surg. Res.* **122,** 145–149
21. Hyogo, H., Roy, S., and Cohen, D. E. (2003) Restoration of gallstone susceptibility by leptin in C57BL/6J ob/ob mice. *J. Lipid Res.* **44,** 1232–1240
22. Subramanian, S., Goodspeed, L., Wang, S., Kim, J., Zeng, L., Ioannou, G. N., Haigh, W. G., Yeh, M. M., Kowdley, K. V., O'Brien, K. D., Pennathur, S., and Chait, A. (2011) Dietary cholesterol exacerbates hepatic steatosis and inflammation in obese LDL receptor-deficient mice. *J. Lipid Res.* **52,** 1626–1635
23. Van Rooyen, D. M., Larter, C. Z., Haigh, W. G., Yeh, M. M., Ioannou, G., Kuver, R., Lee, S. P., Teoh, N. C., and Farrell, G. C. (2011) Hepatic free cholesterol accumulates in obese, diabetic mice and causes nonalcoholic steatohepatitis. *Gastroenterology* **141,** 1393–1403, 1403.e1–5
24. Méndez-González, J., Julve, J., Rotllan, N., Llaverias, G., Blanco-Vaca, F., and Escolà-Gil, J. C. (2011) ATP-binding cassette G5/G8 deficiency causes hypertriglyceridemia by affecting multiple metabolic pathways. *Biochim. Biophys. Acta* **1811,** 1186–1193
25. Liu, J., Sabeva, N. S., Bhatnagar, S., Li, X. A., Pujol, A., and Graf, G. A. (2010) ABCD2 is abundant in adipose tissue and opposes the accumulation of dietary erucic acid (C22:1) in fat. *J. Lipid Res.* **51,** 162–168
26. Ozcan, U., Yilmaz, E., Ozcan, L., Furuhashi, M., Vaillancourt, E., Smith, R. O., Görgün, C. Z., and Hotamisligil, G. S. (2006) Chemical chaperones reduce ER stress and restore glucose homeostasis in a mouse model of type 2 diabetes. *Science* **313,** 1137–1140
27. Newberry, E. P., Xie, Y., Kennedy, S., Han, X., Buhman, K. K., Luo, J., Gross, R. W., and Davidson, N. O. (2003) Decreased hepatic triglyceride accumulation and altered fatty acid uptake in mice with deletion of the liver fatty acid-binding protein gene. *J. Biol. Chem.* **278,** 51664–51672
28. Djouadi, F., Bonnefont, J. P., Thuillier, L., Droin, V., Khadom, N., Munnich, A., and Bastin, J. (2003) Correction of fatty acid oxidation in carnitine palmitoyl transferase 2-deficient cultured skin fibroblasts by bezafibrate. *Pediatr. Res.* **54,** 446–451
29. Devries-Seimon, T., Li, Y., Yao, P. M., Stone, E., Wang, Y., Davis, R. J., Flavell, R., and Tabas, I. (2005) Cholesterol-induced macrophage apoptosis requires ER stress pathways and engagement of the type A scavenger receptor. *J. Cell Biol.* **171,** 61–73
30. Malhi, H., and Kaufman, R. J. (2011) Endoplasmic reticulum stress in liver disease. *J. Hepatol.* **54,** 795–809
31. Du, K., Herzig, S., Kulkarni, R. N., and Montminy, M. (2003) TRB3: a tribbles homolog that inhibits Akt/PKB activation by insulin in liver. *Science* **300,** 1574–1577
32. Yu, L., Hammer, R. E., Li-Hawkins, J., Von Bergmann, K., Lutjohann, D., Cohen, J. C., and Hobbs, H. H. (2002) Disruption of Abcg5 and Abcg8 in mice reveals their crucial role in biliary cholesterol secretion. *Proc. Natl. Acad. Sci. U.S.A.* **99,** 16237–16242
33. Wilund, K. R., Yu, L., Xu, F., Hobbs, H. H., and Cohen, J. C. (2004) High-level expression of ABCG5 and ABCG8 attenuates diet-induced hypercholesterolemia and atherosclerosis in Ldlr−/− mice. *J. Lipid Res.* **45,** 1429–1436
34. Brufau, G., Groen, A. K., and Kuipers, F. (2011) Reverse cholesterol transport revisited: contribution of biliary versus intestinal cholesterol excretion. *Arterioscler. Thromb. Vasc. Biol.* **31,** 1726–1733
35. de Bari, O., Neuschwander-Tetri, B. A., Liu, M., Portincasa, P., and Wang, D. Q. (2012) Ezetimibe: its novel effects on the prevention and the treatment of cholesterol gallstones and nonalcoholic fatty liver disease. *J. Lipids* **2012,** 302847
36. Botham, K. M., and Bravo, E. (1995) The role of lipoprotein cholesterol in biliary steroid secretion. Studies with *in vivo* experimental models. *Prog. Lipid Res.* **34,** 71–97
37. Dikkers, A., and Tietge, U. J. (2010) Biliary cholesterol secretion: more than a simple ABC. *World J. Gastroenterol.* **16,** 5936–5945
38. Kozarsky, K. F., Donahee, M. H., Rigotti, A., Iqbal, S. N., Edelman, E. R., and Krieger, M. (1997) Overexpression of the HDL receptor SR-BI alters plasma HDL and bile cholesterol levels. *Nature* **387,** 414–417
39. Acton, S., Rigotti, A., Landschulz, K. T., Xu, S., Hobbs, H. H., and Krieger, M. (1996) Identification of scavenger receptor SR-BI as a high density lipoprotein receptor. *Science* **271,** 518–520
40. Wiersma, H., Gatti, A., Nijstad, N., Kuipers, F., and Tietge, U. J. (2009) Hepatic SR-BI, not endothelial lipase, expression determines biliary cholesterol secretion in mice. *J. Lipid Res.* **50,** 1571–1580
41. Shetty, S., Eckhardt, E. R., Post, S. R., and van der Westhuyzen, D. R. (2006) Phosphatidylinositol-3-kinase regulates scavenger receptor class B type I subcellular localization and selective lipid uptake in hepatocytes. *Arterioscler. Thromb. Vasc. Biol.* **26,** 2125–2131